ResearchGate

See discussions, stats, and author profiles for this publication at: https://www.researchgate.net/publication/41396675

# The Structural Characteristics of Nonspecific Lipid Transfer Proteins Explain Their Resistance to Gastroduodenal Proteolysis

**ARTICLE** *in* BIOCHEMISTRY · MARCH 2010

Impact Factor: 3.02 · DOI: 10.1021/bi901939z · Source: PubMed

CITATIONS
24

READS
53

**10 AUTHORS**, INCLUDING:

Ramani Wijesinha-Bettoni
Food and Agriculture Organization of the Un…
**13** PUBLICATIONS **237** CITATIONS
SEE PROFILE

Ana Sancho
EB House Austria, University Hospital Salzburg
**46** PUBLICATIONS **1,235** CITATIONS
SEE PROFILE

Syed Umer Abdullah
United Arab Emirates University
**9** PUBLICATIONS **60** CITATIONS
SEE PROFILE

Alan Robert Mackie
Institute of Food Research
**189** PUBLICATIONS **4,795** CITATIONS
SEE PROFILE

Available from: Yuri Alexeev
Retrieved on: 25 January 2016

2130 *Biochemistry* **2010,** *49,* 2130–2139
DOI: 10.1021/bi901939z

BIOCHEMISTRY
including biophysical chemistry & molecular biology
*Article*

# The Structural Characteristics of Nonspecific Lipid Transfer Proteins Explain Their Resistance to Gastroduodenal Proteolysis[†]

Ramani Wijesinha-Bettoni,[‡,⊥] Yuri Alexeev,[§,⊥] Phil Johnson,[§] Justin Marsh,[∥] Ana I. Sancho,[§] Syed U. Abdullah,[§] Alan R. Mackie,[§] Peter R. Shewry,[∥] Lorna J. Smith,*[,‡] and E. N. Clare Mills[§]

[‡]*Department of Chemistry, Inorganic Chemistry Laboratory, University of Oxford, South Parks Road, Oxford OX1 3QR, U.K.,* [§]*Institute of Food Research, Norwich Research Park, Colney NR4 7UA, U.K., and* [∥] *Rothamsted Research, Rothamsted, Harpenden, Herts AL5 2JQ, U.K.* [⊥]*These authors contributed equally to this work*

*Received November 11, 2009; Revised Manuscript Received January 29, 2010*

ABSTRACT: The structure and stability of the allergenic nonspecific lipid transfer protein (LTP) of peach were compared with the homologous LTP1 of barley and its liganded form LTP1b. All three proteins were resistant to gastric pepsinolysis and were only slowly digested at 1 to 2 out of 14 potential tryptic and chymotryptic cleavage sites under duodenal conditions. Peach LTP was initially cleaved at Tyr79-Lys80 and then at Arg39-Thr40 (a site lost in barley LTP1). Molecular dynamics simulations of the proteins under folded conditions showed that the backbone flexibility is limited, explaining the resistance to duodenal proteolysis. Arg39 and Lys80 side chains were more flexible in simulations of peach compared with barley LTP1. This may explain differences in the rates of cleavage observed experimentally for the two proteins and suggests that the flexibility of individual amino acid side chains could be important in determining preferred proteolytic cleavage sites. In order to understand resistance to pepsinolysis, proteins were characterized by NMR spectroscopy at pH 1.8. This showed that the helical regions of both proteins remain folded at this pH. NMR hydrogen exchange studies confirmed the rigidity of the structures at acidic pH, with barley LTP1 showing some regions with greater protection. Collectively, these data suggest that the rigidity of the LTP scaffold is responsible for their resistance to proteolysis. Gastroduodenal digestion conditions do not disrupt the 3D structure of peach LTP, explaining why LTPs retain their ability to bind IgE after digestion and hence their allergenic potential.

Plant nonspecific lipid transfer proteins (LTPs)[1] are a family of low molecular mass (7−9 kDa) basic proteins which were first discovered over 30 years ago when they were thought to play a role in the intracellular trafficking of lipids (*1*). Their precise biological role in plants still remains a matter of debate, but it is now considered more likely they play a role in the transport of monomers involved in the formation of protective hydrophobic cutin and/or suberin layers and the defense of plants against microbial pathogens (*2*). They share a conserved disulfide skeleton with other members of the prolamin superfamily, namely, the 2S albumin storage proteins of dicotyledonous seeds and α-amylase/trypsin inhibitors of cereal grains (*3*). However, the disulfide connectivities in the LTP family are different to those in the 2S albumins and inhibitors, allowing the bundle of four α-helices that makes up their basic scaffold to form a hydrophobic cavity into which a variety of lipophilic molecules, including lipids, can bind (*2*). The three-dimensional structures of a number of LTPs have been described including a crystal structure of peach LTP (*4*) and solution structures of the barley LTP1 in an unliganded form (*5*) and complexed with various ligands (*6*). In addition, a modified form of barley LTP1, termed LTP1b (*7*), in which an adduct is attached to the protein via the Asp7 side chain has been identified in both barley seeds and in beer. While it was originally proposed that the adduct was *cis*-7-heptadecenoic acid (*8*), subsequent investigations have shown that it is α-ketol 9-hydroxy-10-oxo-12(*Z*)-octadecenoic acid (*9*). NMR studies showed the adduct lies in the LTP1 cavity of LTP1b, displacing Tyr79 and increasing protein mobility (*10*).

More recently, LTPs have been designated as a family of pan allergens (*11*, *12*), causing severe allergies to a variety of foods, including peach. Indeed, peach LTP accounts for sensitization in more than 90% of patients allergic to peach in the Mediterranean area and can cause severe, life-threatening reactions including anaphylaxis (*13*). There are also reports of cereal LTPs causing allergic reactions following consumption of wheat-based foods (*14*) and beer (*15*) although these allergies probably result from primary sensitization toward peach LTP. It is thought that allergenic LTPs in food are able to sensitize via the gastrointestinal tract due to their stability to digestion (*16*) and thus trigger severe allergic reactions. Stability to digestion may allow a protein to be presented to the gastrointestinal immune system in an immunologically active form (*17*).

While there has been a general assumption that the structural stability of LTPs contributes to their resistance to digestion, this

[†]This work is funded by the EC FP6 project EuroPrevall (FOOD-CT-2005-514000) and the BBSRC competitive strategic grants to IFR and Rothamsted Research. The work of S.A. on this project is supported by a grant from the Higher Education Commission, Pakistan.

*Address correspondence to this author. Phone: +44 1865 272694. Fax: +44 1865 272690. E-mail: lorna.smith@chem.ox.ac.uk.

[1]Abbreviations: COSY, $^1$H−$^1$H correlation spectroscopy; LTP, nonspecific lipid transfer protein; MALDI-TOF, matrix-assisted laser desorption ionization/time of flight; MALDI-MS, matrix-assisted laser desorption ionization mass spectrometry; NOESY, nuclear Overhauser enhancement spectroscopy; RMSF, root-mean-square fluctuation; TOCSY, total correlation spectroscopy.

 Published on Web 02/02/2010 © 2010 American Chemical Society

has not been fully explained at a molecular level. Correlation between flexibility and proteolytic sites has been established in previous studies. Fontana et al. (*18*) proposed that accessibility and flexibility of the polypeptide chain at the site of proteolytic attack promote optimal binding and proper interaction with protease. The theory is supported by reported correlation of main chain temperature factors of thermolysin with proteolytic cleavage sites. Falconi et al. (*19*) found that enhanced chain flexibility indicated by molecular dynamics simulations is the key feature of proteolytic cleavage site. Out of 14 solvent-accessible proteolytic sites in superoxide dismutase, only one flexible site is cleaved.

It is possible that subtle differences in the dynamical properties of proteins sharing the same three-dimensional structure affect their stability to digestion. We have therefore compared the structure of the allergenic LTP of peach (also designated as the allergen Pru p 3) with the homologous LTP1 of barley, together with its modified form LTP1b (*9*). We have also characterized the effects of conditions which are relevant to those found in the gastrointestinal tract (such as pH) on LTP folding and dynamics and related the structures of the proteins to their patterns of gastroduodenal proteolysis.

## EXPERIMENTAL PROCEDURES

*Protein Preparations*. Peach LTP was purified from the skin of peach fruits by a combination of ammonium sulfate fractionation and cation exchange chromatography according to Gaier et al. (*20*). Barley LTP and LTP1b were prepared as described by Wijesinha-Bettoni et al. (*10*).

*Simulated Gastric and Duodenal Proteolysis*. Proteins (0.25 mg/mL in the final digestion mix) were incubated with pepsin (1:20 w/w) at pH 2.5 to simulate gastric proteolysis, followed by trypsin and chymotrypsin (1:400:100 w/w/w) at pH 6.5 to mimic duodenal proteolysis, as described by Moreno et al. (*21*). The enzyme activities were 3300 units/mg of protein calculated using hemoglobin as substrate, 13800 units/mg of protein using BAEE as substrate, and 44 units/mg of protein using BTEE as substrate for pepsin, trypsin, and bovine R-chymotrypsin, respectively. Progress of proteolysis was followed by SDS−PAGE analysis under reducing conditions with 0.5 M dithiothreitol using a 12% Bis-Tris gel in a NuPAGE system (Invitrogen, Groningen, The Netherlands) according to the manufacturer's instructions. Proteins were visualized by Sypro Ruby staining (Invitrogen, Groningen, The Netherlands). Marker proteins were insulin A chain ($M_r$ 2500), insulin B chain ($M_r$ 3500), aprotinin ($M_r$ 6000), lysozyme ($M_r$ 14400), trypsin inhibitor ($M_r$ 21500), carbonic anhydrase ($M_r$ 31000), lactate dehydrogenase ($M_r$ 36500), glutamic dehydrogenase ($M_r$ 55400), BSA ($M_r$ 66300), phosphorylase B ($M_r$ 97400), $\beta$-galactosidase ($M_r$ 116300), and myosin ($M_r$ 200000) (Invitrogen, Groningen, The Netherlands).

For N-terminal sequencing, the duodenal proteolysis products were separated by SDS−PAGE electrophoresis and electroblotted onto PVDF membrane (Immobilon-$P^{SQ}$), and the protein was stained with SimplyBlue colloidal Coomassie (Invitrogen, Groningen, The Netherlands), as described by Maciercenka et al. (*22*). N-Terminal sequencing (Edman degradation) was performed for selected peptides at the Protein and Nucleic Acid Chemistry Facility, Department of Biochemistry at University of Cambridge (Cambridge, U.K.).

Digestion products were also analyzed by MALDI-TOF mass spectrometry. Each sample was mixed with a saturated sinapinic acid (Sigma-Aldrich, Dorset, U.K.) matrix in 30% (v/v) acetonitrile and 0.1% (v/v) trifluoroacetic acid (TFA). The target plates used were polished stainless steel (Bruker Daltonics, Coventry, U.K.). Samples were prepared in the presence or absence of 5 mM tris(2-carboxyethyl)phosphine (TCEP) depending upon whether reduction was required. Approximately 0.5 $\mu$L of the sample/matrix mixture was spotted onto the MALDI target and dried in air. The MALDI-MS measurements were performed using a Bruker UltraFlex MALDI-TOF/TOF mass spectrometer (Bruker Daltonics, Coventry, U.K.) equipped with a pulsed $N_2$ laser ($\lambda$ = 337 nm, frequency 10 Hz). Whole protein spectra were recorded over the 2000−12000 Da range in linear mode at an accelerating voltage of 25 kV by averaging of at least 300 individual laser shots. The concentration of each protein solution was adjusted to give peak intensity similar to that of the calibrants used. Calibration was performed using ACTH (adrenocorticotropic hormone), somatostatin, ubiquitin, insulin, and myoglobin. Data analysis was performed by comparison of experimentally derived peptide masses with those predicted by *in silico* digestion of peach and barley LTPs by trypsin and chymotrypsin using the Mmass software package (*23*) with a 200 ppm tolerance.

*Molecular Dynamics Simulations*. The structures for simulations were the barley LTP1 first NMR structure in 1LIP (*5*) (determined at pH 4.0, 310 K) and the peach LTP X-ray structure 2ALG (*4*) (pH 6.5, 293 K). The peach 2ALG structure is a dimer; since peach LTP is monomeric at neutral and low pH (*20*) and both polypeptides were similar, chain A was chosen for simulations. Modeling was undertaken without ligands, and crystallographic water molecules were excluded in the simulations. All calculations were carried out using the programs CHARMM (version c34b2) (*24*) and NAMD (version 2.6) (*25*). All-atom version 27 CHARMM force field parameters (*26*) were employed. Polar hydrogens were introduced with the CHARMM HBUILD command (*24*, *27*). A sphere of preequilibrated TIP3 water molecules was centered on the center of mass of the protein to form a 10 Å shell of water molecules around the protein. All water molecules overlapping with the protein were deleted. Structures were minimized with conjugate gradient and line search algorithms implemented in NAMD for 10000 steps without any constraints on the protein and water molecules. Subsequently, the temperature of the simulation was raised from 0 to 250 K in 50 K steps (50 ps each) and then from 250 to 300 K in 10 K steps (50 ps each). Finally, the system was equilibrated for 500 ps. Water molecules were kept within the sphere by a weak spherical harmonic boundary potential. The CHARMM default cutoffs for long-range interactions were used; i.e., a shift function was used for the electrostatic term with a cutoff at 12 Å, and a switch truncation acting between 10 and 12 Å was employed for the van der Waals interactions. Temperature was controlled using Langevin dynamics with a damping constant of 5 $ps^{-1}$, with hydrogen atoms uncoupled to the heat bath. The integration time step was set to 2 fs. The protein coordinates were extracted from the equilibrated MD trajectory (5 ns) every 4 ps for the following RMS deviation and fluctuations analysis. The backbone atoms (atom types Cα, C, N, O) were reoriented to remove translational and rotational modes.

*NMR Studies*. The NMR studies were carried out at pH 1.85, 310 K. The barley LTP1 assignments were taken from the published data (*5*) and were confirmed for the present conditions. The assignments for peach LTP were obtained using 2D spectra and could be confirmed for 96% of the protein sequence and have been deposited (BioMagRes bank accession code 16294).

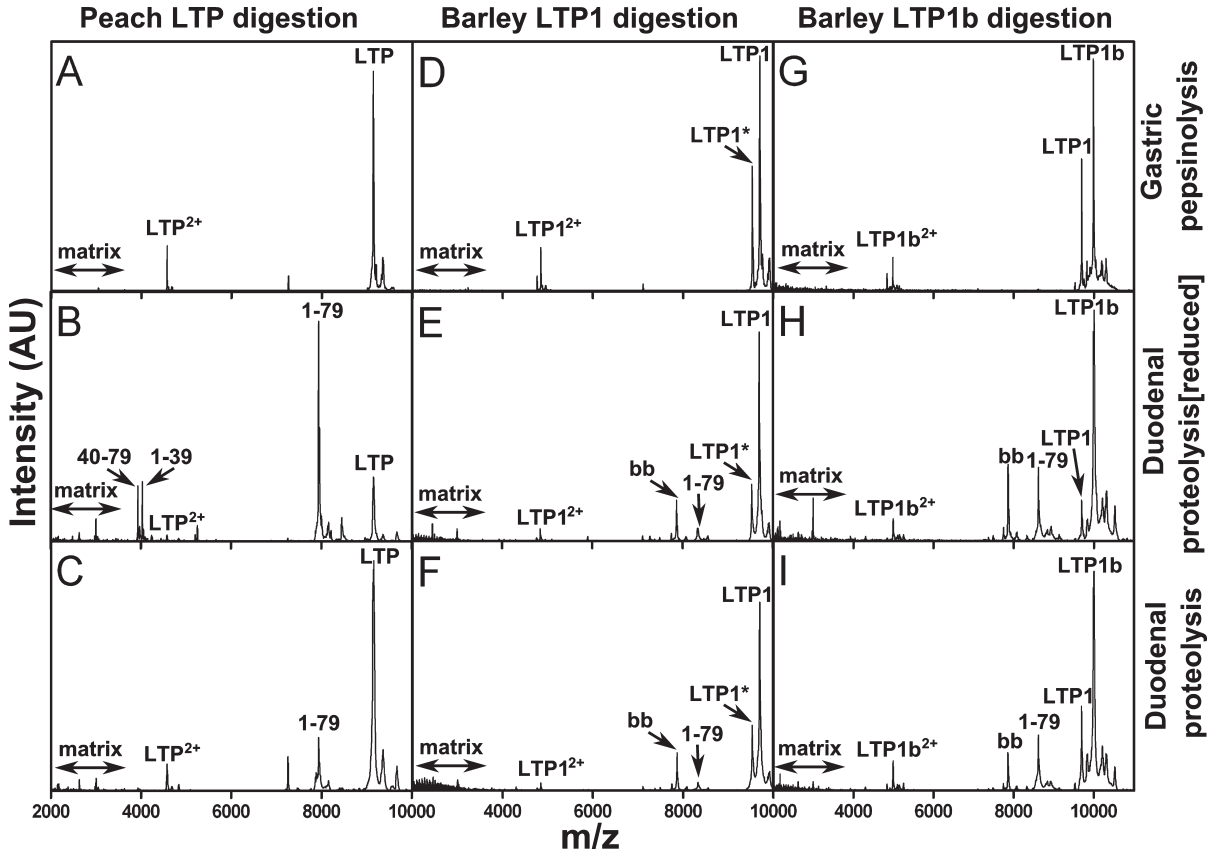


FIGURE 1: Analysis of LTP gastroduodenal digestion by MALDI-TOF mass spectrometry: panels A−C, peach LTP digestion; panels D−F, barley LTP1 digestion; panels G−I, barley LTP1b digestion. Spectra are as follows: A, D, G, after 60 min gastric pepsinolysis; B, E, H, 60 min pepsinolysis followed by 30 min duodenal proteolysis (reduced); C, F, I, 60 min pepsinolysis followed by 30 min duodenal proteolysis (nonreduced). Intact (undigested) protein is labeled as LTP (peach), LTP1 (barley LTP1), or LTP1b (barley LTP1b). Low intensity mass events of approximately 3000 Da were frequently observed and were most likely matrix-associated. Mass events are singly charged unless denoted as 2+. bb represents Bowman−Birk inhibitor added to terminate duodenal proteolysis.

The data were of good quality, although four peaks cannot be assigned as they are not visible in the spectra under the experimental conditions.

All spectra were collected using home-built spectrometers at the Department of Biochemistry, Oxford University, functioning at 500, 600, or 750 MHz, using protein samples ranging from 2 to 3 mM concentration in 95%/5% $H_2O/D_2O$. DQF-COSY, TOCSY, and NOESY spectra were recorded for barley LTP1 at pH 4, 310 K, and pH 5, 298 K, and TOCSY and phase-sensitive COSY (phCOSY) spectra at pH 1.8, 310 K. For peach LTP, phCOSY, DQF-COSY, TOCSY, and NOESY spectra were recorded at pH 5.3 at 310 K and phCOSY, TOCSY, and NOESY spectra at pH 5.3, 298 K; further spectra were collected at pH 4, 298 K, which included a NOESY spectrum in 95%/5% $H_2O/D_2O$, NOESY and TOCSY spectra in $D_2O$ (showing slowly exchanging amides), and reverse hydrogen exchange NOESY and TOCSY spectra (fully exchanged sample freeze-dried and redissolved in $H_2O$). Sets of TOCSY, NOESY, and phCOSY spectra were also recorded at pH 6.5, 293 K, and pH 1.8, 37 °C. Further NOESY spectra were collected at pH 3.9, 298 K, and pH 3, 293 K. All TOCSY spectra collected had mixing times in the range 72−74 ms, and the NOESY spectra had 200 ms mixing times. Spectra were collected in both the absence and presence of 50 mM NaCl (which did not make a noticeable difference to the spectral quality).

For NMR hydrogen exchange experiments on barley LTP1 and peach LTP, the proteins were dissolved in $H_2O$ at pH 1.85 and freeze-dried prior to hydrogen exchange. The samples were then dissolved to 3 mM in 25 mM deuterated sodium acetate buffer (pH 1.85). A series of nine COSY spectra was collected for each protein at 310 K. Acquisition was started 1 h after dissolution in $D_2O$, and the acquisition time was 7.8 h per spectrum.

## RESULTS

*Gastroduodenal Proteolysis*. Peach LTP, barley LTP1, and barley LTP1b were all completely resistant to gastric pepsinolysis at pH 2.5, as shown by MALDI-TOF mass spectrometry (Figure 1A,D,G) over the mass range of 2000−12,000 Da and SDS−PAGE (Figure 2). The masses of all three proteins did not alter throughout the time course of pepsinolysis studied. A 9144.2 Da peptide was observed throughout pepsin digestion of peach LTP, which corresponds to residues 1−91 of intact, unmodified peach protein (Swiss Prot Q9LED1). Following mass spectrometry analysis it became evident that the barley LTP1 (9694.4 Da, accession number P07597) preparation was contaminated by LTP1 without a C-terminal tryptophan which is represented in spectra as a mass of 9529.5 Da. Loss of the C-terminal residue of barley LTP has been observed previously in purified preparations (*6*). Digests of barley LTP1 gave a fragment mass of 9694.4 Da corresponding to the calculated intact mass of 9694.89 Da for barley LTP1 (Swiss Prot P07597) (Figure 1D) and barley LTP1b a dominant mass of 9990.2 Da. This corresponds to LTP1 with the addition of 294.5 Da, consistent with the

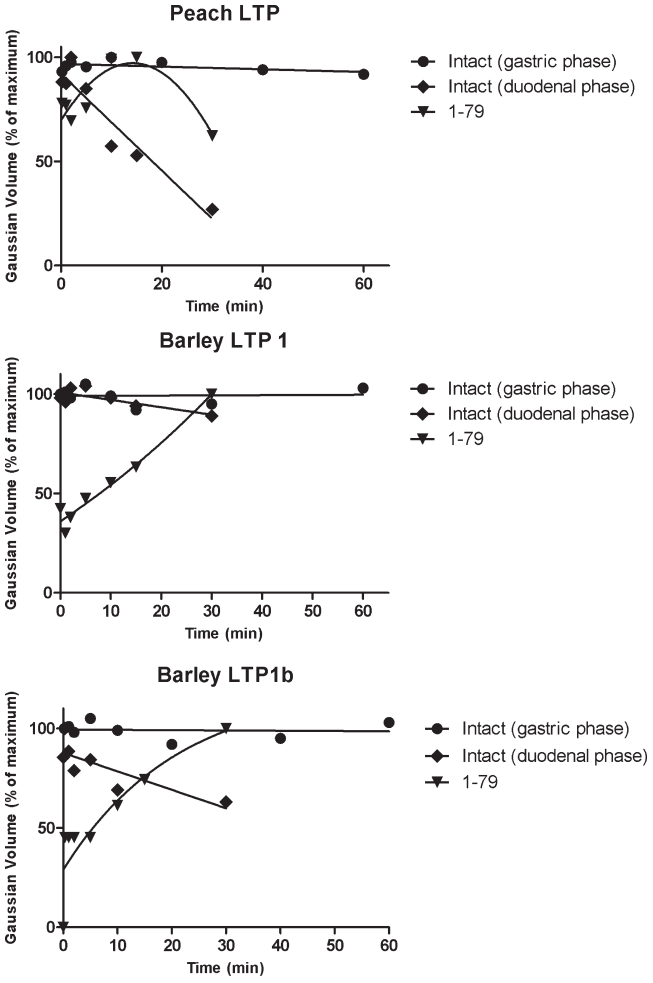


FIGURE 2: Relative abundance of LTPs and digestion products over time as estimated from densitometry of SDS−PAGE gels. Band intensities were calculated as a percentage of maximum Gaussian volume by scanning of gel images and subsequent analysis using the TotalLab package. Curve fitting was performed using the Prism package (version 5.01). In the case of peach LTP the identity of the 1−79 fragment was confirmed by N-terminal sequence analysis (not shown) and MALDI-TOF data (Table 1). In the case of barley LTP1 and LTP1b N-terminal sequence information for the major fragment was unobtainable because of low abundance, and identity of the 1−79 fragment was inferred as it was the only fragment of significant abundance in the MALDI-TOF experiments.

modification of Asp7 with α-ketol 9-hydoxy-10-oxo-12(*Z*)-octadecanoic acid as previously reported (*9*) with a calculated mass of 9989.9 Da.

Following gastric pepsinolysis, the digestion of peach and barley LTPs by trypsin and chymotrypsin under duodenal conditions was followed by MALDI-MS (Figure 1) and SDS−PAGE (Figure 2), with the masses determined for the proteolysis products being compared with those of peptides predicted by *in silico* digestion with chymotrypsin and trypsin using mMass (*23*). No digestion of peach LTP, barley LTP1, and barley LTP1b was observed by either SDS−PAGE (Figure 2) or MALDI-MS (Figure 1A,D,G) during the gastric (pepsinolysis) phase. For duodenal digestion results were consistent between experimental methods, with quantitative analysis by SDS−PAGE showing that peach LTP was more rapidly digested than either of the barley LTPs and the unliganded barley LTP1 being the most resistant LTP, (Figure 2). Concentration of peptide 1−79 rises over time except for peach LTP where it drops after an initial rise which is consistent with further digestion to 1−39 and

Table 1: Peach and Barley LTP Digestion Products Identified by MALDI-TOF Mass Spectrometry[a]

| sequence assignment | obsd *m*/*z* (Da) | calcd *m*/*z* (Da) | error (ppm) |
|---|---|---|---|
| Peach LTP, Accession Number Q9LED1 | | | |
| 1−91 (LTP) | 9144.2 | 9145.0 | 83 |
| 40−79 | 3929.9 | 3930.5 | 165 |
| 1−39 | 4028.6 | 4028.6 | 17 |
| 1−79 | 7939.7 | 7940.1 | 50 |
| Barley LTP1, Accession Number P07597 | | | |
| 1−91 (LTP1) | 9694.4 | 9694.9 | 51 |
| 1−90 (LTP1*) | 9530.8 | 9533.2 | 248 |
| 1−79 | 8329.6 | 8331.4 | 213 |
| Barley LTP1b, Accession Number P07597 | | | |
| 1−91 (LTP1b) | 9990.2 | 9989.9 | 30 |
| 1−79 | 8624.8 | 8625.4 | 115 |

[a]Proteins and peptides are denoted in the same way as that shown in Figure 1. Putative peptides were assigned on the basis of matching masses observed by MALDI-TOF and predicted masses calculated using mMass.

40−79 fragments. Smaller (1−39 and 40−79) fragments are not observed using SDS−PAGE, possibly because of their small size (< 4000 Da) and relatively low abundance. Fourteen different tryptic and chymotryptic digestion sites are theoretically possible for peach LTP, using established cleavage rules for trypsin and chymotrypsin. These cleavage sites were used to generate a list of peptides and corresponding masses under the assumption that any number of missed cleavages were possible. This list of potential proteolytic fragments was searched against experimentally obtained MALDI data using the "match data" function of mMass using an accepted tolerance of 200 ppm. This showed that only two of the potential tryptic and chymotryptic cleavage sites were cleaved in the simulated duodenal digest. For peach LTP a mass of 9144.2 Da corresponding to the intact protein was observed throughout duodenal digestion, together with a 7939.7 Da polypeptide digestion product (Figure 1B,C). This mass corresponds to the predicted chymotryptic digestion product residues 1−79 (Table 1) and is consistent with the fact that N-terminal sequencing of the dominant $M_r$ 7 kDa fragment resolved by SDS−PAGE, which increased in abundance early during digestion and then began to decrease after 30 min (Figure 2 A), possessed an intact N-terminus. Relatively less intense signals corresponding to lower masses were observed in increasing amounts as duodenal digestion progressed. These were consistent with the presence of peptides corresponding to residues 1−39 and 40−79, which may result from further digestion of the dominant 7939.7 Da peptide. Thus, after initial cleavage of peach LTP between Tyr79 and Lys80 by chymotrypsin, the resulting 7940 Da polypeptide is cleaved between Arg39 and Thr40 by trypsin. All of the observed fragments were greatly reduced in relative intensity when the digests were not reduced using TCEP prior to MALDI-MS (Figure 1), suggesting that most of the fragments remain associated by intramolecular disulfide bridges (see Figure 3). However, the presence of observable 1−79 peptide in the nonreduced samples indicates either that some fragments are unassociated after duodenal digestion or that the ionization used in the MALDI experiments partially fragments associated peptides. A mass of 7258.18 Da was observed in peach protein preparations and could not be assigned to possible proteolysis products or other known components of the reaction mixture.

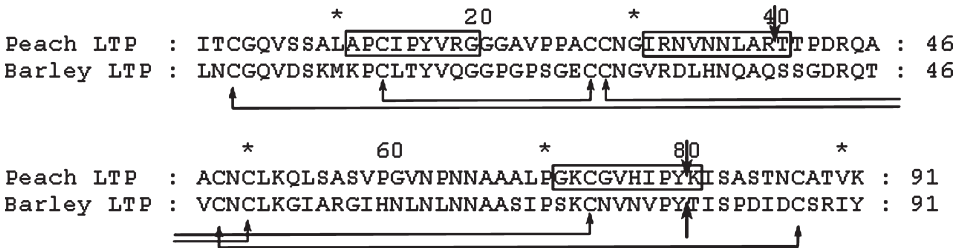


FIGURE 3: Sequence alignment of peach LTP and barley LTP1. Peach IgE-binding epitopes (*33*) are shown in boxes. The actual cleavage sites determined by mass spectrometry are shown by arrows, trypsin cleaving at Arg39-Thr40 and chymotrypsin at Tyr79-Lys80. Disulfide bonds are indicated by arrows.

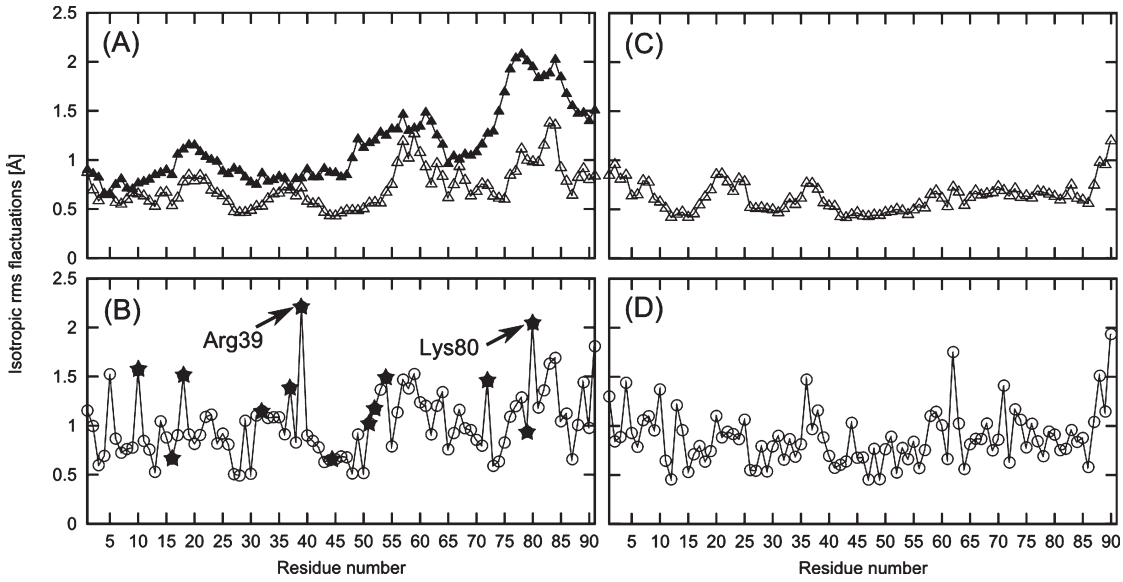


FIGURE 4: RMS fluctuations of peach LTP (A and B) and barley LTP1 (C and D). Cα atom fluctuations are marked by ▲ (from *B*-factors) and △ (from simulations); all atom fluctuations are marked by ○ (from simulations). Residues 39 and 80 are labeled on panel B. For peach LTP the RMS fluctuations were calculated from the X-ray *B*-factors using the formula $B = (8\pi^2/3)\Delta r^2$. Potential cleavage sites are marked by black stars on panel B.

Similarly, other minor peaks (unmarked peaks in Figure 1) were occasionally present in spectra but could not be assigned.

Similar analysis of digested barley LTP1 revealed that the intact protein was present in all digestion samples corresponding to a mass of 9694.4 Da. A digestion product of 8329.6 Da was observed in duodenal digests after 15 and 30 min but was of very low abundance (Figure 1 F). This can be tentatively assigned as corresponding to residues 1−79 (expected mass 8331.38 Da) as the mass accuracy of the measurement was poor (200 ppm) due to the low abundance. The relative abundance of this 8331.38 Da chymotryptic digestion product increased throughout digestion (Figure 2B), but in contrast to the major digestion products of the peach LTP, its abundance in MALDI-MS analysis was not affected by reduction (Figure 1E−F). For barley LTP1b a fragment of mass 8624.8 Da was observed after 10 min of duodenal digestion, which was presumed to correspond to residues 1−79 (expected mass of 8625.38 Da) with the addition of the 294.5 Da adduct (Figure 1I). The relative abundance of this fragment also increased up to 30 min while the abundance of the intact protein decreased, as observed by SDS−PAGE (Figure 2C). As with barley LTP1, the relative abundance of this fragment did not appear to change significantly under reducing conditions (Figure 1H−I).

Thus, all three types of LTP were all completely resistant to simulated gastric proteolysis, and of 14 possible cleavages in duodenal proteolysis, only 2 were observed (Figure 3). Of the seven conserved cleavage sites in the peach and barley LTPs, only one (Lys80) was cleaved in all proteins, and this occurred more slowly in barley LTPs than in peach LTP.

*Molecular Dynamics Simulations*. Since all proteases require some flexibility in their substrates, particularly pepsin (*28*), the dynamic properties of the peach and barley LTPs were studied computationally in order to seek an explanation for their experimentally observed resistance to proteolysis. MD simulations were run for peach LTP and barley LTP1. Over a 5 ns simulation time the structures of both proteins were stable. The Cα atom and all-atom positional root-mean-square deviations through the simulations were higher for barley LTP1 compared to peach LTP by approximately 1 Å (barley LTP1, Cα atom RMSD 2.2 Å, all-atom RMSD 2.7 Å; peach LTP, Cα atom RMSD 1.2 Å, all-atom RMSD 1.6 Å). However, care must be taken in drawing conclusions about these differences, as different methods were used for structural determination of the two proteins (NMR for barley LTP1, X-ray crystallography for peach LTP) and the protein conformations may have been affected by the purification methods used. The isotropic RMS fluctuations of the Cα atoms and all atoms were calculated from the MD trajectories to monitor any difference in the flexibility of the LTP structure in the simulations (see Figure 4). For comparison, atomic fluctuations were estimated from the experimental *B*-factors from the crystal structure of peach LTP. There is generally a good correlation between the simulation RMS

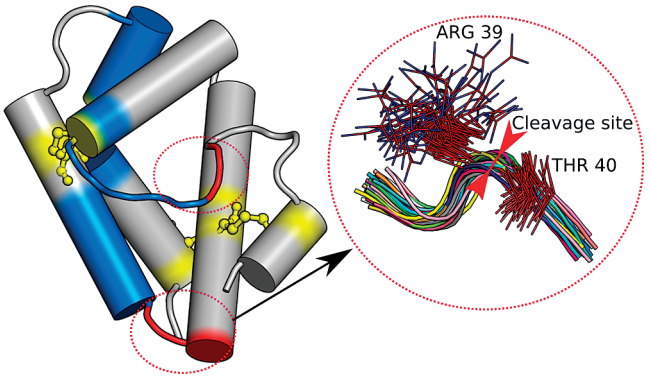


FIGURE 5: A schematic view of the structure of peach LTP. The cleavage sites Arg39-Thr40 and Tyr79-Lys80 are colored red. IgE-binding epitopes are colored blue. On the right side in the circle is the overlay of 50 snapshots of Arg39-Thr40 side chain coordinates taken from MD trajectory shown as sticks with backbone atoms of neighboring residues shown as tubes. Hydrogen atoms are not shown; carbon and nitrogen atoms are colored red and blue, respectively. The structures were reoriented to remove translational and rotational motions.

fluctuations and those calculated from the *B*-factors (correlation coefficient 0.6, Figure 4A). Any differences may reflect the fact that the X-ray structure of peach LTP was determined for a dimeric form of the protein while the simulations of peach LTP used just one monomer. Our analysis of peach LTP and barley LTP1 revealed both to be monomeric at both pH 3.0 and pH 7.0 (data not shown), indicating that changes in oligomeric state did not play a significant role in protease protection in our experiments and that use of a monomeric structure in our simulations was appropriate.

Overall, the RMS fluctuations seen in both simulations are low. This is consistent with the experimentally observed resistance of these proteins to proteolysis. However, there are two regions in peach LTP that have Cα atom RMSF values greater than 1.0 Å, namely, residues 56−61 and 78−85 (Figure 4A). The second of these regions also shows higher experimental Cα *B*-factors (RMSF values calculated from the *B*-factors greater than 1.5 Å for residues 74−88). In contrast, the only significant backbone flexibility observed in barley LTP1 is at the C-terminus (residues 87−91, Figure 4C). In addition, the all-atom RMSF values show that several side chains are very flexible, namely, Arg39 and Lys80 of peach LTP (Figures 4B and 5) and Ile90 at the C-terminus of barley LTP1 (Figure 4D) which have RMS fluctuations >1.9 Å. Thus, the two gastroduodenal proteolysis sites observed in peach LTP, Arg39−Thr40 (trypsin) and Tyr79−Lys80 (chymotrypsin), both have highly mobile side chains directly adjacent to them. Both cleavage sites are shown in Figure 5. The trypsin cleavage site is shown in great detail, particularly, the Arg39 flexible side chain. This flexibility presumably enables access to the peptide bond and hence cleavage. For barley LTP1 gastroduodenal proteolysis only cleaves the 79−80 peptide bond, the tryptic site having been lost through substitution of Arg for Gln at position 39 in barley compared with peach LTP (Figure 3). However, cleavage of the 79−80 peptide bond was much slower in barley LTP1 compared to peach LTP and may result from the lower backbone mobility of this region in the barley protein seen in the Cα atom RMSF data (Figure 4B) alone or in combination with the change in amino acid sequence close to the cleavage site (Lys80 in peach LTP vs Thr80 in barley LTP1).

The increased susceptibility to chymotryptic cleavage of barley LTP1b compared to barley LTP1 at the 79−80 peptide bond implies that there is increased exposure or flexibility of these residues when the lipid-like α-ketol 9-hydoxy-10-oxo-12(*Z*)-octadecanoic acid adduct is present. This is interesting in the light of our previous NMR studies of barley LTP1b which showed that the lipid-like adduct lies in the hydrophobic cavity of the protein, with Tyr79 being displaced to accommodate the ligand (*10*). In addition, the modified barley LTP1b showed a reduced level of hydrogen exchange protection compared to barley LTP1, presumably reflecting a loosening of the protein structure and increased flexibility (*10*). These changes would be consistent with the increased susceptibility of barley LTP1b over barley LTP1 to duodenal digestion reported in this work. Moreover, the chemical shift changes for residues 77−81 observed on binding palmitate and palmityl-CoA (*6*, *29*) to barley LTP1 suggest that changes in Tyr79 orientation and increasing side chain flexibility may be a general feature of occupation of the binding cavity in LTP1 by a suitably sized ligand. If this is the case, the digestibility of LTP1 may be explained by changes in Tyr79 orientation which may be influenced by binding different types of ligands (adduct versus noncovalently bound ligand).

*NMR Spectroscopic Study at Low pH*. The MD simulations show that the LTP structures have limited dynamical behavior under native conditions at pH 7. This may be responsible at least in part for their resistance to chymotrypsin and trypsin proteolysis. However, to understand the experimentally observed resistance to pepsinolysis, the proteins need to be characterized at low pH (conditions under which many proteins are substantially unfolded). Peach LTP and barley LTP1 were therefore studied by NMR spectroscopy at pH 1.8 and 310 K. The assignments for peach LTP were obtained using 2D spectra and have been deposited (BioMagRes bank accession code 16294). The data were of good quality, although four peaks (Leu54, Ser55, Ile81, and Ser82) cannot be seen in the spectra under the experimental conditions and thus could not be assigned. In general, the resonances of residues in the second part of helix C, which includes residues Leu54 and Ser55, proved particularly difficult to assign. It is likely that this region of the protein has some internal dynamics which gives rise to exchange broadening of the resonances. This is consistent with the preliminary 1D NMR studies of peach LTP by Gaier et al. (*30*), which suggested that minor unstructured regions are present at pH 3. Support for this also comes from the increased RMS fluctuations and *B*-factors for this region seen in the MD simulations and crystal structure of peach LTP under native conditions (Figure 4).

A comparison of the backbone NH chemical shifts between pH 1.8 and pH 5.3 (spectra at 310 K at both pH values) for peach LTP is shown in Figure 6A. Only Thr 40 shows a difference greater than 0.2 ppm, with Asp43 showing the next largest difference of 0.16 ppm. The barley LTP1 assignments were taken from the published data (*5*) and were confirmed for the present conditions. A comparison of the backbone NH chemical shifts at pH 1.8 and pH 4 is shown in Figure 6B. The residues with NH shift differences greater than 0.2 ppm are Glu26, Gln39, Ser40, Asp86, Ser88, Arg89, and Ile90 in barley LTP1. The differences in Hα chemical shifts were all smaller than 0.15 ppm.

To determine whether the observed NH chemical shift differences were due to the proximity of these NH groups to Asp and Glu side chains or to the C-terminus (all of which will change their protonation states over the pH range studied), the structures

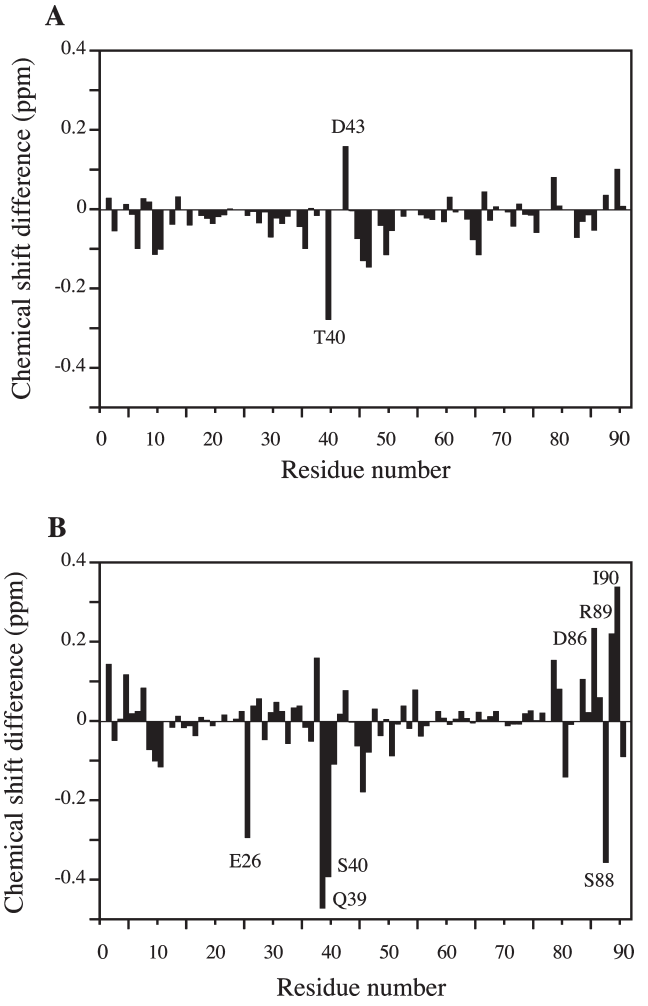


FIGURE 6: Histograms showing the $^1$H chemical shift difference (low pH minus high pH) for backbone NH groups at 37 °C: (A) pH 1.8 and pH 5 for peach LTP and (B) pH 1.8 and pH 4 for barley LTP1. Residues whose NH groups show a difference > 0.2 ppm are labeled.

of peach LTP (2ALG, molecule B crystal structure which has a ligand partially inserted in the cavity, pH 6.5, 293 K) and barley LTP1 (1LIP, NMR structure, pH 4, 310 K) were analyzed. Peach LTP has only one ionizable residue, Asp43, which would explain the lack of pronounced differences in NH shift under the different pH conditions. Barley LTP1 has five Asp residues and one Glu residue. For peach LTP, the NH of Thr40, the only amide proton showing a significant pH shift, is only 2.75 Å away from OD2 of Asp43. For barley LTP1, nearly all of the amide protons showing large changes in chemical shift with pH are either those of Asp or Glu residues themselves or are closer than 3.5 Å to the OD or OE groups in Asp or Glu side chains in the protein structure. The only exception is the NH of Ile90, whose nitrogen atom is, however, close to the C-terminus oxygen. Thus all of the significant changes in chemical shift for peach LTP and barley LTP1 at low pH come from changes in electrostatic interactions arising from changes in protonation state of adjacent side chains or the protein C-terminus. There is no evidence for changes to the protein structure or significant unfolding at pH 1.8.

*Low pH Hydrogen Exchange NMR Study*. Although there is no evidence from the chemical shift data for changes to the LTP structures at low pH, the proteins may become more flexible under these conditions. In order to probe the dynamics of the protein structures at low pH, we studied the hydrogen exchange protection of individual backbone amide protons in peach LTP and barley LTP1. A number of residues in both proteins are strongly protected, even under this extreme pH condition (Figure 7), particularly residues in the helices (Figure 8). This level of hydrogen exchange is typical of that expected for a protein which is still fully folded and has fairly limited internal dynamics. The hydrogen exchange data show that most of the epitopic regions in peach LTP retain their hydrogen-bonded secondary structure (the backbone amide protons of residues 14, 17, 30−34, 36, 37, 44−47, 49, 69, and 71−75 all show some degree of protection from hydrogen exchange) and are folded at the pH found in the stomach.

However, the hydrogen exchange protection in peach LTP was on average lower than in barley LTP1, with significant differences in certain parts of the protein. After 1 h of dissolving the protein in $D_2O$, barley LTP1 has 31 protected amides, compared with 24 for peach LTP. There was a pronounced difference between the protection in the two proteins by the last time point, 63.5 h after dissolution, with barley LTP containing 20 strongly protected amides while peach contained only 8 (panel D vs panel B of Figure 7). The main differences (Figure 8) lie in the second part of helix C (residues 51−56), the start of helix D (residues 65−67), and the loop connecting these two helices (residues 58 and 60), which show far greater protection in barley LTP. Although differences in the observed protection could reflect differences in the intrinsic hydrogen exchange rates for the two protein sequences in these regions, comparisons of the intrinsic exchanges rates show that this is not a significant factor here. As two of the unassigned residues in peach LTP (Leu54 and Ser55) also lie in this region, it is likely that internal dynamics within the protein structure may be giving rise to exchange broadening. Hence, there is evidence from the hydrogen exchange data that the peach LTP structure is somewhat more flexible than the barley LTP1 structure under low pH conditions. This, together with the higher RMS fluctuations seen for some regions of the peach LTP structure in the MD simulations, may explain the fact that peach LTP is slightly more susceptible to gastroduodenal proteolysis than barley LTP1.

## DISCUSSION

In this paper, we have succeeded in relating the structural stabilities of peach and barley LTPs to their stabilities toward gastric pepsinolysis at pH 2.5 and simulated gastroduodenal proteolysis at pH 6.5. Despite the presence in each protein of numerous predicted pepsin, trypsin, and chymotrypsin cleavage sites, peach LTP was only cleaved at two sites, by trypsin (Arg39-Thr40) and chymotrypsin (Tyr79-Arg80), while barley LTP was cleaved only at the chymotryptic site, as the tryptic site has been lost as a consequence of substitution of the Arg for Gln at position 39 in barley LTP. Molecular dynamics simulations under conditions where the proteins are fully folded showed that backbone flexibility is mainly limited to the C-terminus, with side chain mobility at residues 39 and 80 promoting cleavage at/near these sites in peach LTP. The slightly higher susceptibility to duodenal proteolysis for peach LTP compared to barley LTP1 can be ascribed to its increased structural flexibility, as seen from the NMR hydrogen exchange data. This conclusion is further supported by a comparison of the gastroduodenal proteolysis of barley LTP1 and the liganded form barley LTP1b. The latter, which is known to have a more flexible structure, is again seen to be slightly more susceptible to proteolysis. The results also show that the peptides resulting from duodenal digestion of LTPs remain disulfide linked to the remainder of the protein. Thus,

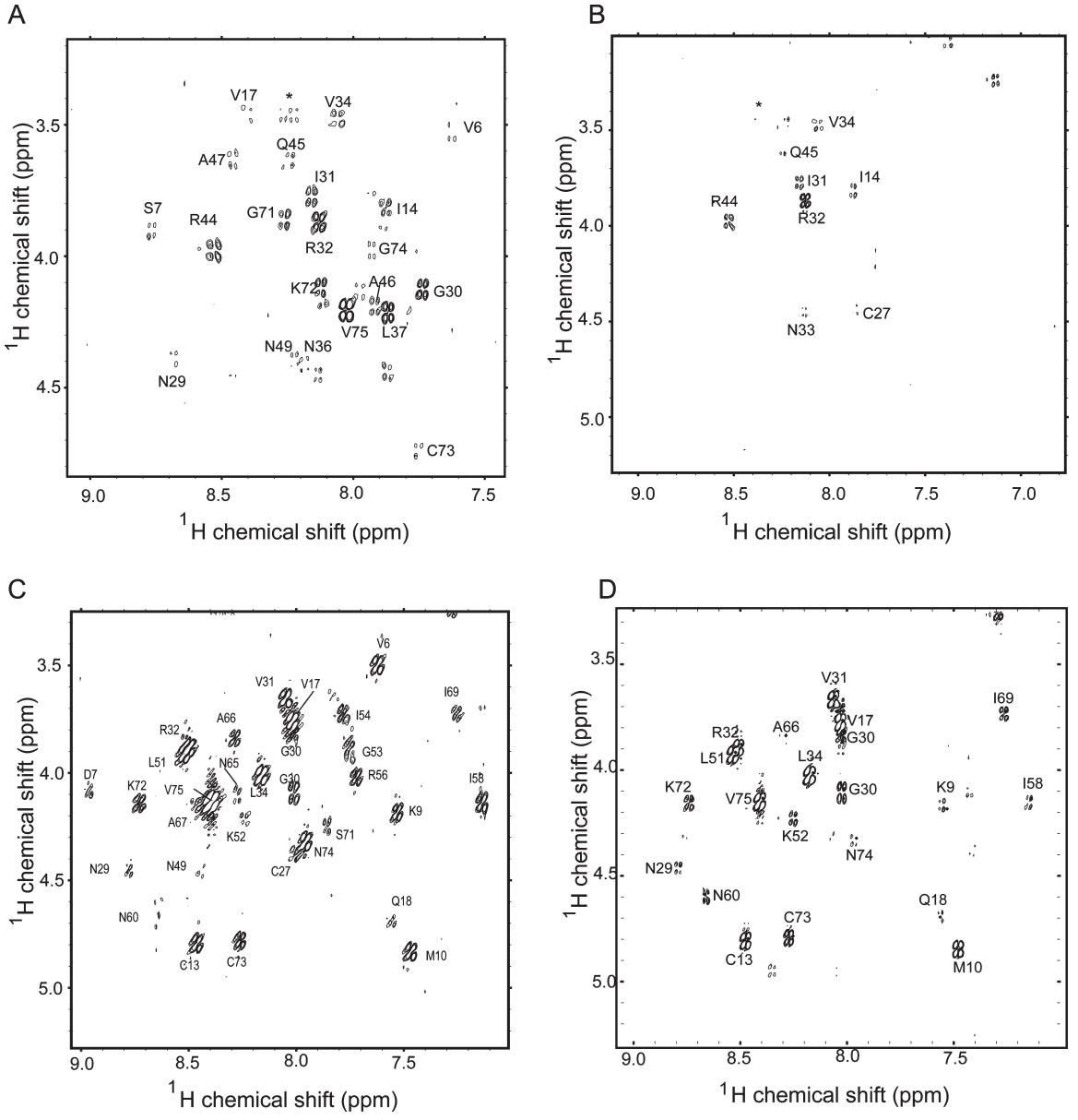


FIGURE 7: The fingerprint regions of 2D COSY spectra showing amide protons that are protected from hydrogen exchange in peach LTP (A, B) and barley LTP1 (C, D) at pH 1.8 and 37 °C. (A) and (C) are spectra collected 1 h after the proteins were dissolved in $D_2O$, while (B) and (D) are spectra collected 62 h after dissolution in $D_2O$.

gastrointestinal digestion does not result in the diffusion of digested peptides from the protein scaffold. The effect of this proteolytic "clipping" of LTP on protein structure is of great interest and will be investigated further.

The experimental and theoretical work was performed on unliganded LTPs (barley LTP1b adduct is not technically a ligand because it is covalently attached to the protein) in this work. It is certainly possible that ligand binding may affect protein flexibility and hence protein digestion. In particular, ligand binding may affect the orientation of Tyr79 in the C-terminal region which may influence chymotrypsin binding. For example, Tyr79 in barley LTP1 is the most buried and least flexible, which may result in poor susceptibility to duodenum digestion as seen in the mass spectrometry data (see Figure 1). Additional work is under way in our laboratory to investigate the effect of ligand binding on structure and digestion.

The retention of the overall three-dimensional structure of these proteins following simulated gastrodudoenal digestion explains the fact that simulated gastric (*31*) and gastrointestinal proteolysis does not affect the ability of allergenic LTPs, such as grape, to bind IgE and elicit histamine release (*32*). Epitope mapping employing overlapping synthetic peptides has shown that major IgE epitopes of peach LTP lie between residues 11−25, 31−45, and 71−80 with mimotope analysis confirming the involvement of regions around residues 34−46 and 76−79 in IgE binding (*33*). Both the Arg39-Thr40 and the Tyr79-Arg80 intestinal endoprotease cleavage sites of peach LTP lie within these major IgE-binding regions, the latter site lying at the C-terminal end of the 76−79 epitope region (see Figure 5). Even after cleavage our analysis indicates that LTP proteolysis products will remain assembled in an intact-like structure retaining the native topology and, hence, not affecting the IgE epitope structures, providing the disulfide bonds are maintained in their oxidized form. Similarly, T-cell epitopes of peach LTP are not generally hydrolyzed during simulated gastrointestinal proteolysis, with the exception of the major T-cell epitope that spans residues 34−48 (*34*) and hence contains within it the Arg39-Thr40 cleavage site. Thus, while it appears that the T-cells

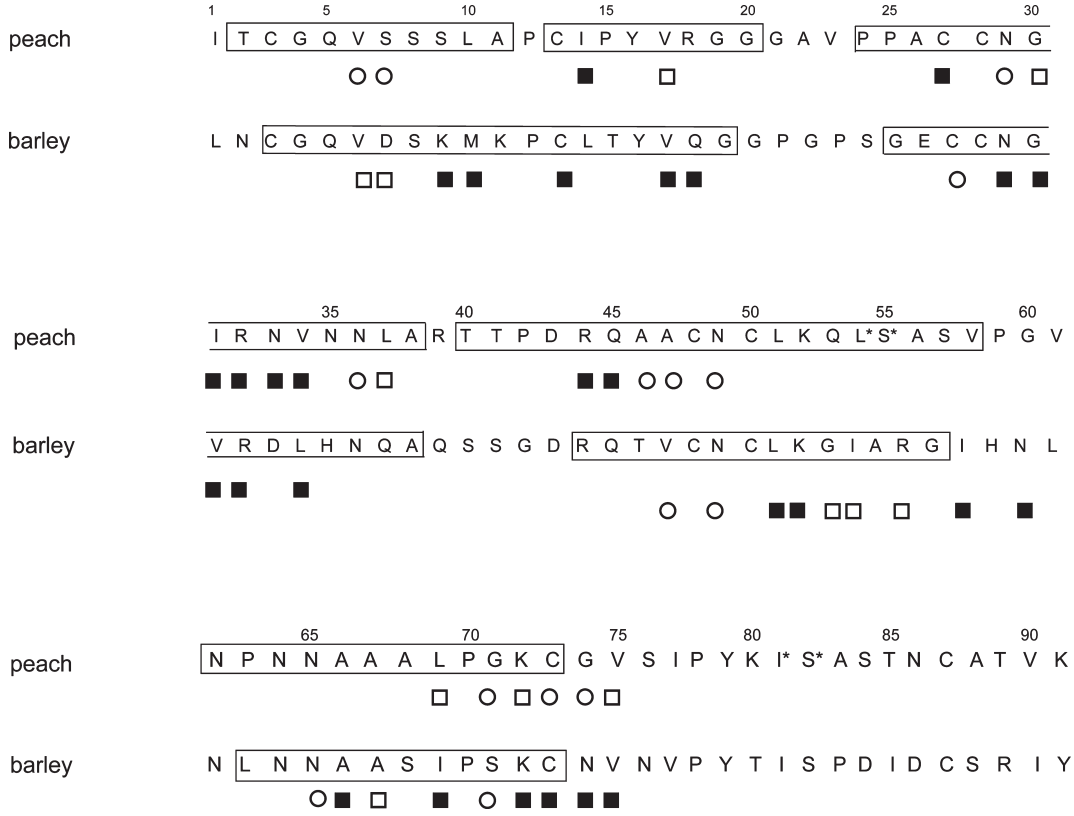


FIGURE 8: Hydrogen exchange protection of backbone amide protons for peach LTP and barley LTP1 at pH 1.8, 37 °C. Amide proton exchange is shown with open circles, open squares, and filled squares representing amide protons present in a spectrum collected 1 h (weakly protected), 16.6 h (protected), and 63.5 h (strongly protected), respectively, after dissolution of the protein in $D_2O$. Residues marked with an asterisk represent unassigned residues in peach LTP. Regions of α-helix are framed at the sequence positions.

involved in generating IgE responses to peach originate from the gut, this evidence indicates that the immune systems of peach-allergic individuals are primed to some extent to intact peach LTP.

It is interesting to note the colocation of the endoprotease cleavage sites and IgE epitopes in the loops spanning residues 39−43 (loop 2) and 74−91 (unstructured region), which may reflect the fact that, like immunoglobulin binding sites, proteases require a certain degree of flexibility in the docking with a target protein. Indeed, the ability of aspartyl proteases to bind to extended regions of polypeptides and unfolded or partially folded proteins in a chaperone-like manner has recently been characterized (*35*). Since LTPs maintain a tightly folded compact structure at low pH, they will present little of their polypeptide backbone in a manner that would allow pepsin to bind and hence explaining the lack of hydrolysis of these proteins by pepsin. Trypsin and chymotrypsin have a lower requirement for substrates presenting peptide bonds in an extended conformation but do require some level of flexibility. Hence only those candidate cleavage sites lying in the more mobile regions of the protein toward the C-terminus are actually cleaved. These data also demonstrate the limitations of simplistic tools such as PeptideCutter for predicting proteolytic cleavage of intact proteins as they do not take account of the properties of folded proteins in determining patterns of proteolysis.

Our research supports the theory (*18*, *19*) that accessibility and flexibility of proteolytic cleavage sites are key factors for proteolysis. We found that not only is the flexibility of the backbone important but also the flexibility of amino acid side chains participating in proteolysis. This study confirms the important role of protein flexibility in proteolysis and expands the scope of study to food allergens, where digestion is a key component of antigen reactivity.

## ACKNOWLEDGMENT

The authors thank Neil Rigby and Mike Naldrett for experimental support in the work.

## REFERENCES

1. Kader, J. C. (1996) Lipid-transfer proteins in plants. *Annu. Rev. Plant Physiol. Plant Mol. Biol. 47*, 627–654.
2. Douliez, J. P., Michon, T., Elmorjani, K., and Marion, D. (2000) Structure, biological and technological functions of lipid transfer proteins and indolines, the major lipid binding proteins from cereal kernels. *J. Cereal Sci. 32*, 1–20.
3. Jenkins, J. A., Griffiths-Jones, S., Shewry, P. R., Breiteneder, H., and Mills, E. N. C. (2005) Structural relatedness of plant food allergens with specific reference to cross-reactive allergens: An in silico analysis. *J. Allergy Clin. Immunol. 115*, 163–170.
4. Pasquato, N., Berni, R., Folli, C., Folloni, S., Cianci, M., Pantano, S., Helliwell, J. R., and Zanotti, G. (2006) Crystal structure of peach Pru p 3, the prototypic member of the family of plant non-specific lipid transfer protein pan-allergens. *J. Mol. Biol. 356*, 684–694.
5. Heinemann, B., Andersen, K. V., Nielsen, P. R., Bech, L. M., and Poulsen, F. M. (1996) Structure in solution of a four-helix lipid binding protein. *Protein Sci. 5*, 13–23.
6. Lerche, M. H., and Poulsen, F. H. (1998) Solution structure of barley lipid transfer protein complexed with palmitate. Two different binding modes of palmitate in the homologous maize and barley non-specific lipid transfer proteins. *Protein Sci. 7*, 2490–2498.
7. Bakan, B., Hamberg, M., Larue, V., Prange, T., Marion, D., and Lascombe, M. B. (2009) The crystal structure of oxylipin-conjugated barley LTP1 highlights the unique plasticity of the hydrophobic cavity of these plant lipid-binding proteins. *Biochem. Biophys. Res. Commun. 390*, 780–785.
8. Lindorff-Larsen, K., Lerche, M. H., Poulsen, F. M., Roepstorff, P., and Winther, J. R. (2001) Barley lipid transfer protein, LTP1, contains

a new type of lipid-like post-translational modification. *J. Biol. Chem. 276*, 33547–33553.
9. Bakan, B., Hamberg, M., Perrocheau, L., Maume, D., Rogniaux, H., Tranquet, O., Rondeau, C., Blein, J. P., Ponchet, M., and Marion, D. (2006) Specific adduction of plant lipid transfer protein by an allene oxide generated by 9-lipoxygenase and allene oxide synthase. *J. Biol. Chem. 281*, 38981–38988.
10. Wijesinha-Bettoni, R., Gao, C. L., Jenkins, J. A., Mackie, A. R., Wilde, P. J., Mills, E. N. C., and Smith, L. J. (2007) Post-translational modification of barley LTP1b: The lipid adduct lies in the hydrophobic cavity and alters the protein dynamics. *FEBS Lett. 581*, 4557–4561.
11. Sanchez-Monge, R., Lombardero, M., Garcia-Selles, F. J., Barber, D., and Salcedo, G. (1999) Lipid-transfer proteins are relevant allergens in fruit allergy. *J. Allergy Clin. Immunol. 103*, 514–519.
12. Pastorello, E. A., Farioli, L., Pravettoni, V., Ortolani, C., Ispano, M., Monza, M., Baroglio, C., Scibola, E., Ansaloni, R., Incorvaia, C., and Conti, A. (1999) The major allergen of peach (*Prunus persica*) is a lipid transfer protein. *J. Allergy Clin. Immunol. 103*, 520–526.
13. Fernandez-Rivas, M., Bolhaar, S., Gonzalez-Mancebo, E., Asero, R., van Leeuwen, A., Bohle, B., Ebner, C., Rigby, N., Sancho, A. I., Miles, S., Zuidmeer, L., Knulst, A., Breiteneder, H., Mills, C., Hoffmann-Sommergruber, K., and van Ree, R. (2006) Apple allergy across Europe: How allergen sensitization profiles determine the clinical expression of allergies to plant foods. *J. Allergy Clin. Immunol. 118*, 481–488.
14. Pastorello, E. A., Farioli, L., Conti, A., Pravettoni, V., Bonomi, S., Iametti, S., Fortunato, D., Scibilia, J., Bindslev-Jensen, C., Ballmer-Weber, B., Robino, A. M., and Ortolani, C. (2007) Wheat IgE-mediated food allergy in European patients: alpha-amylase inhibitors, lipid transfer proteins and low-molecular-weight glutenins—Allergenic molecules recognized by double-blind, placebo-controlled food challenge. *Int. Arch. Allergy Immunol. 144*, 10–22.
15. Garcia-Casado, G., Crespo, J. F., Rodriguez, J., and Salcedo, G. (2001) Isolation and characterization of barley lipid transfer protein and protein Z as beer allergens. *J. Allergy Clin. Immunol. 108*, 647–649.
16. Asero, R., Mistrello, G., Roncarolo, D., de Vries, S. C., Gautier, M. F., Ciurana, L. F., Verbeek, E., Mohammadi, T., Knul-Brettlova, V., Akkerdaas, J. H., Bulder, I., Aalberse, R. C., and van Ree, R. (2000) Lipid transfer protein: A pan-allergen in plant-derived foods that is highly resistant to pepsin digestion. *Int. Arch. Allergy Immunol. 122*, 20–32.
17. Mills, E. N. C., Jenkins, J. A., Alcocer, M. J. C., and Shewry, P. R. (2004) Structural, biological, and evolutionary relationships of plant food allergens sensitizing via the gastrointestinal tract. *Crit. Rev. Food Sci. Nutr. 44*, 379–407.
18. Fontana, A., Fassina, G., Vita, C., Dalzoppo, D., Zamai, M., and Zambonin, M. (1986) Correlation between sites of limited proteolysis and segmental mobility in thermolysin. *Biochemistry 25*, 1847–1851.
19. Falconi, M., Parrilli, L., Battistoni, A., and Desideri, A. (2002) Flexibility in monomeric Cu,Zn superoxide dismutase detected by limited proteolysis and molecular dynamics simulation. *Proteins: Struct., Funct., Genet. 47*, 513–520.
20. Gaier, S., Marsh, J., Oberhuber, C., Rigby, N. M., Lovegrove, A., Alessandri, S., Briza, P., Radauer, C., Zuidmeer, L., van Ree, R., Hemmer, W., Sancho, A. I., Mills, C., Hoffmann-Sommergruber, K., and Shewry, P. R. (2008) Purification and structural stability of the peach allergens Pru p 1 and Pru p 3. *Mol. Nutr. Food Res. 52* (Suppl. 2), S220–S229.
21. Moreno, F. J., Mellon, F. A., Wickham, M. S. J., Bottrill, A. R., and Mills, E. N. C. (2005) Stability of the major allergen Brazil nut 2S albumin (Ber e 1) to physiologically relevant in vitro gastrointestinal digestion. *FEBS J. 272*, 341–352.
22. Macierzanka, A., Sancho, A. I., Mills, E. N. C., Rigby, N. M., and Mackie, A. R. (2009) Emulsification alters simulated gastrointestinal proteolysis of beta-casein and beta-lactoglobulin. *Soft Matter 5*, 538–550.
23. Strohalm, M., Hassman, M., Kosata, B., and Kodicek, M. (2008) mMass data miner: An open source alternative for mass spectrometric data analysis. *Rapid Commun. Mass Spectrom. 22*, 905–908.
24. Brooks, B. R., Bruccoleri, R. E., Olafson, B. D., States, D. J., Swaminathan, S., and Karplus, M. (1983) Charmm—A program for macromolecular energy, minimization, and dynamics calculations. *J. Comput. Chem. 4*, 187–217.
25. Phillips, J. C., Braun, R., Wang, W., Gumbart, J., Tajkhorshid, E., Villa, E., Chipot, C., Skeel, R. D., Kale, L., and Schulten, K. (2005) Scalable molecular dynamics with NAMD. *J. Comput. Chem. 26*, 1781–1802.
26. MacKerell, A. D., Bashford, D., Bellott, M., Dunbrack, R. L., Evanseck, J. D., Field, M. J., Fischer, S., Gao, J., Guo, H., Ha, S., Joseph-McCarthy, D., Kuchnir, L., Kuczera, K., Lau, F. T. K., Mattos, C., Michnick, S., Ngo, T., Nguyen, D. T., Prodhom, B., Reiher, W. E., Roux, B., Schlenkrich, M., Smith, J. C., Stote, R., Straub, J., Watanabe, M., Wiorkiewicz-Kuczera, J., Yin, D., and Karplus, M. (1998) All-atom empirical potential for molecular modeling and dynamics studies of proteins. *J. Phys. Chem. B 102*, 3586–3616.
27. Brunger, A. T., and Karplus, M. (1988) Polar hydrogen positions in proteins—Empirical energy placement and neutron-diffraction comparison. *Proteins: Struct., Funct., Genet. 4*, 148–156.
28. Fruton, J. S. (1974) Active-site of pepsin. *Acc. Chem. Res. 7*, 241–246.
29. Lerche, M. H., Kragelund, B. B., Bech, L. M., and Poulsen, F. M. (1997) Barley lipid-transfer protein complexed with palmitoyl CoA: The structure reveals a hydrophobic binding site that can expand to fit both large and small lipid-like ligands. *Structure 5*, 291–306.
30. Gaier, S., Oberhuber, C., Rigby, N., Marsh, J., Hemmer, W., Mills, C., Shewry, P., Scheiner, O., and Hoffmann-Sommergruber, K. (2008) Allergenicity of peach allergens Pru p 1 and Pru p 3 related with protein stability. *Allergy 63*, 572–572.
31. Asero, R. (1999) Detection and clinical characterization of patients with oral allergy syndrome caused by stable allergens in Rosaceae and nuts. *Ann. Allergy Asthma Immunol. 83*, 377–383.
32. Vassilopoulou, E., Rigby, N., Moreno, F. J., Zuidmeer, L., Akkerdaas, J., Tassios, I., Papadopoulos, N. G., Saxoni-Papageorgiou, P., van Ree, R., and Mills, C. (2006) Effect of in vitro gastric and duodenal digestion on the allergenicity of grape lipid transfer protein. *J. Allergy Clin. Immunol. 118*, 473–480.
33. Pacios, L. F., Tordesillas, L., Cuesta-Herranz, J., Compes, E., Sanchez-Monge, R., Palacin, A., Salcedo, G., and Diaz-Perales, A. (2008) Mimotope mapping as a complementary strategy to define allergen IgE-epitopes: Peach Pru p 3 allergen as a model. *Mol. Immunol. 45*, 2269–2276.
34. Schulten, V., Radakovics, A., Hartz, C., Mari, A., Vazquez-Cortes, S., Fernandez-Rivas, M., Lauer, I., Jahn-Schmid, B., Eiwegger, T., Scheurer, S., and Bohle, B. (2009) Characterization of the allergic T-cell response to Pru p 3, the nonspecific lipid transfer protein in peach. *J. Allergy Clin. Immunol. 124*, 100–107.
35. Hulko, M., Lupas, A. N., and Martin, J. (2007) Inherent chaperone-like activity of aspartic proteases reveals a distant evolutionary relation to double-c barrel domains of AAA-ATPases. *Protein Sci. 16*, 644–653.